Neuroscience 119 (2003) 481–496

COMPARATIVE ANALYSIS OF FATTY ACID AMIDE HYDROLASE AND CB_1 CANNABINOID RECEPTOR EXPRESSION IN THE MOUSE BRAIN: EVIDENCE OF A WIDESPREAD ROLE FOR FATTY ACID AMIDE HYDROLASE IN REGULATION OF ENDOCANNABINOID SIGNALING

M. EGERTOVÁ,[a] B. F. CRAVATT[b] AND M. R. ELPHICK[a]*

[a]*School of Biological Sciences, Queen Mary, University of London, London E1 4NS, UK*

[b]*The Skaggs Institute for Chemical Biology and Departments of Cell Biology and Chemistry, The Scripps Research Institute, La Jolla, CA 92037, USA*

Abstract—Fatty acid amide hydrolase (FAAH) catalyses hydrolysis of the endocannabinoid arachidonoylethanolamide ("anandamide") *in vitro* and regulates anandamide levels in the brain. In the cerebellar cortex, hippocampus and neocortex of the rat brain, FAAH is located in the somata and dendrites of neurons that are postsynaptic to axon fibers expressing the CB_1 cannabinoid receptor [Proc R Soc Lond B 265 (1998) 2081]. This complementary pattern of FAAH and CB_1 expression provided the basis for a hypothesis that endocannabinoids may function as retrograde signaling molecules at synapses in the brain [Proc R Soc Lond B 265 (1998) 2081; Phil Trans R Soc Lond 356 (2001) 381] and subsequent experimental studies have confirmed this [Science 296 (2002) 678]. To assess more widely the functions of FAAH in the brain and the potential impact of FAAH activity on the spatiotemporal dynamics of endocannabinoid signaling in different regions of the brain, here we have employed immunocytochemistry to compare the distribution of FAAH and CB_1 throughout the mouse brain, using $FAAH^{-/-}$ mice as negative controls to validate the specificity of FAAH-immunoreactivity observed in wild type animals. In many regions of the brain, a complementary pattern of FAAH and CB_1 expression was observed, with FAAH-immunoreactive neuronal somata and dendrites surrounded by CB_1-immunoreactive fibers. In these regions of the brain, FAAH may regulate postsynaptic formation of anandamide, thereby influencing the spatiotemporal dynamics of retrograde endocannabinoid signaling. However, in some regions of the brain such as the globus pallidus and substantia nigra pars reticulata, CB_1 receptors are abundant but with little or no associated FAAH expression and in these brain regions the spatial impact and/or duration of endocannabinoid signaling may be less restricted than in regions enriched with FAAH. A more complex situation arises in several regions of the brain where both FAAH and CB_1 are expressed but in a non-complementary pattern, with FAAH located in neurons and/or oligodendrocytes that are proximal but not postsynaptic to CB_1-expressing axon fibers. Here FAAH may nevertheless influence endocannabinoid signaling but more remotely. Finally, there are regions of the brain where FAAH-immunoreactive neurons and/or oligodendrocytes occur in the absence of CB_1-immunoreactive fibers and here FAAH may be involved in regulation of signaling mediated by other endocannabinoid receptors or by receptors for other fatty acid amide signaling molecules. In conclusion, by comparing the distribution of FAAH and CB_1

*Corresponding author. Tel: +44-20-7882-5290; Fax: +44-20-8983-0973.
E-mail address: m.r.elphick@qmul.ac.uk (M. R. Elphick).

Abbreviations: 3V, third ventricle; 4V, fourth ventricle; 12N, hypoglossal nucleus; aca, anterior commissure (anterior); aci, anterior commissure (intrabulbar); Acb, accumbens nucleus; AD, anterodorsal thalamic nucleus; AHC, anterior hypothalamic area (central); AM, anteromedial thalamic nucleus; AOD, anterior olfactory nucleus (dorsal); AOL, anterior olfactory nucleus (lateral); AOM, anterior olfactory nucleus (medial); AON, anterior olfactory nucleus; APir, amygdalopiriform transitional area; ATg, anterior tegmental nucleus; Au, auditory cortex; AV, anteroventral thalamic nucleus; BLA, basolateral amygdaloid nucleus (anterior); BLP, basolateral amygdaloid nucleus (posterior); BLV, basolateral amygdaloid nucleus (ventral); BMP, basomedial amygdaloid nucleus (posterior); CA1, field CA1 of the hippocampus; CA3, field CA3 of the hippocampus; CbCx, cerebellar cortex; cc, corpus callosum; Cg, cingulate cortex; CPu, caudate putamen; D3V, dorsal 3 ventricle; DEn, dorsal endopiriform nucleus; DG, dentate gyrus; DR, dorsal raphe nucleus; DTT, dorsal tenia tecta; Ect, ectorhinal cortex; EP, entopeduncular nucleus; EPl, external plexiform layer of the olfactory bulb; FrA, frontal association cortex; Gl, glomerular layer of the olfactory bulb; GP, globus pallidus; GrDG, granule cell layer of the dentate gyrus; GrL, granule cell layer of the cerebellar cortex; GrO, granule cell layer of the olfactory bulb; Hi, hippocampus; I, insular cortex; IC, inferior colliculus; ICjM, islands of Calleja (Major); icp, inferior cerebellar peduncle; IG, indusium griseum; IO, inferior olive; IOD, inferior olive (dorsal nucleus); IODM, inferior olive (dorsomedial cell group); IOM, inferior olive (medial nucleus); IOPr, inferior olive (principal nucleus); Int, interposed cerebellar nuclei; IntP, interposed cerebellar nucleus (posterior); La, lateral amygdaloid nucleus; LaDL, lateral amygdaloid nucleus (dorsolateral); Lat, lateral cerebellar nuclei; LaVL, lateral amygdaloid nucleus (ventrolateral); LaVM, lateral amygdaloid nucleus (ventromedial); LEnt, lateral entorhinal cortex; LG, lateral geniculate nucleus; LS, lateral septal nucleus; LV, lateral ventricle; M1, primary motor cortex; M2, secondary motor cortex; MD, mediodorsal thalamic nucleus; me5, mesencephalic 5 tract; Me5, mesencephalic 5 nucleus; Med, medial cerebellar nucleus; MedDL, medial cerebellar nucleus (dorsolateral protruberance); Mi, Mitral cell layer of the olfactory bulb; MG, medial geniculate nucleus; ML, molecular layer of the cerebellar cortex; mlf, medial longitudinal fasciculus; MN, mammillary nuclei; MnR, median raphe nucleus; MoDG, molecular layer of the dentate gyrus; MS, medial septal nucleus; mt, mammillothalamic tract; O, orbital cortex; OB, olfactory bulb; ON, olfactory nerve; PaS, parasubiculum; PCL, Purkinje cell layer of the cerebellar cortex; Pir, piriform cortex; Pn, pontine nuclei; Po, posterior thalamic nucleus; PRh, perirhinal cortex; PT, paratenial thalamic nucleus; PtA, parietal association cortex; PrL, prelimbic cortex; PrS, presubiculum; Py, pyramidal tract; Rbd, rhabdoid nuclei; Rt, reticular thalamic nucleus; RS, retrosplenial cortex; S, subiculum; S1, primary somatosensory cortex; S2, secondary somatosensory cortex; SC, superior colliculus; SHi, septohippocampal nucleus; sm, stria medullaris of the thalamus; SNR, substantia nigra pars reticulata; sp5, spinal trigeminal tract; TeA, temporal association cortex; TS, triangular septal nucleus; Tu, olfactory tubercle; V1, primary visual cortex; V2L, secondary visual cortex (lateral area); V2M, secondary visual cortex (medial); VA, ventral anterior thalamic nucleus; VL, ventrolateral thalamic nucleus; VM, ventromedial thalamic nucleus; VP, ventroposterior thalamic nucleus; wm, white matter; xscp, decussation of the superior cerebellar peduncle.

0306-4522/03$30.00+0.00
doi:10.1016/S0306-4522(03)00145-3

in the mouse brain, we have provided a neuroanatomical framework for comparative analysis of the role of FAAH in regulation of the spatiotemporal dynamics of retrograde endocannabinoid signaling in different regions of the brain.

Key words: FAAH, retrograde, anandamide, oleamide, oligodendrocyte.

Fatty acid amide hydrolase (FAAH) is a membrane-associated enzyme that was first isolated from rat liver on account of its ability to catalyze hydrolysis of the sleep-inducing lipid oleamide (Cravatt et al., 1995, 1996). Analysis of the substrate selectivity of FAAH revealed, however, that it also hydrolyzes anandamide (arachidonoylethanolamide), a putative endogenous ligand for the CB_1-type cannabinoid receptor in the brain (Cravatt et al., 1996). 2-Arachidonylglycerol (2-AG), a second putative endocannabinoid, also appears to be reactive with FAAH *in vitro* (Goparaju et al., 1998) and therefore these data indicate that FAAH might be generally required for inactivation of endocannabinoids in the brain. Evidence in support of this was provided by the detection of FAAH in brain tissue and localization of FAAH expression in neurons of the rat brain (Cravatt et al., 1996; Giang and Cravatt, 1997; Thomas et al., 1997; Egertová et al., 1998; Tsou et al., 1998). Moreover, recently mice lacking the FAAH gene have been generated and analysis of these animals has demonstrated that FAAH controls endogenous anandamide levels in the brain and attenuates the behavioral effects of exogenous anandamide (Cravatt et al., 2001). Interestingly, however, analysis of mice lacking FAAH indicates that FAAH is not responsible for regulating 2-AG *in vivo* (Lichtman et al., 2002), and consistent with this idea, the enzyme monoglyceride lipase is now thought to be the main enzyme involved in inactivation of 2-AG in the brain (Dinh et al., 2002).

The potential for FAAH to exert a regulatory influence on endocannabinoid signaling at a synaptic level has been investigated by using immunocytochemistry to compare the distribution of FAAH and the CB_1 receptor in selected regions of the rat brain (Egertová et al., 1998). Importantly, FAAH is localized in the somata and dendrites of principal neurons in the cerebellar cortex (Purkinje cells), hippocampus (pyramidal cells) and the neocortex (pyramidal cells). Moreover, in each of these brain regions there is a complementary pattern of cannabinoid receptor expression, with CB_1 targeted to the axon terminals of neurons that are presynaptic to the FAAH-expressing principal cells. Detection of FAAH in the somato-dendritic compartment of neurons that are postsynaptic to CB_1-expressing axons led us to propose a model of endocannabinoid signaling in which endocannabinoids are both synthesized and inactivated postsynaptically and function as retrograde synaptic messenger molecules that act on presynaptic CB_1 receptors to inhibit release of "classical" neurotransmitters (Egertová et al., 1998; Elphick and Egertová, 2001).

Recently, several studies have demonstrated that endocannabinoids do indeed act as retrograde signals at synapses in the brain (reviewed in Maejima et al., 2001a; Wilson and Nicoll, 2002; Kreitzer and Regehr, 2002). In particular, Wilson and Nicoll (2001) and Ohno-Shosaku et al. (2001) showed that endocannabinoids mediate a retrograde signal from depolarized hippocampal pyramidal cells to presynaptic GABAergic axon terminals that causes suppression of inhibitory input (depolarization-induced suppression of inhibition or DSI). Similarly, Kreitzer and Regehr (2001a) reported that depolarization-induced suppression of excitation (DSE) in the cerebellar cortex is mediated by a retrograde endocannabinoid signal from depolarized Purkinje cells to presynaptic glutamatergic parallel fibers. Because FAAH is expressed in neurons that generate endocannabinoids (e.g. hippocampal pyramidal cells and Purkinje cells; Egertová et al., 1998), it is likely that this enzyme may influence the spatiotemporal dynamics of retrograde signaling by endocannabinoids.

To obtain a complete assessment of FAAH's potential role in the regulation of endocannabinoid signaling, we have performed an immunocytochemical analysis of FAAH and CB_1 expression throughout the mouse brain, using FAAH-knockout mice to establish unequivocally the specificity of FAAH-immunostaining in wild type animals. The detailed analysis of FAAH and CB_1 expression in the mouse brain that we present here provides a neuroanatomical framework that will facilitate use of the mouse as a model system for analysis of the physiological and behavioral roles of the endocannabinoid signaling system.

EXPERIMENTAL PROCEDURES

Preliminary immunocytochemical analysis of FAAH and CB_1 expression was performed using brains from mice of the BALB/c strain to establish working methods prior to analysis of brains from FAAH-knockout mice ($FAAH^{-/-}$) and their wild type littermates ($FAAH^{+/+}$). $FAAH^{-/-}$ and $FAAH^{+/+}$ mice were produced from intercrosses of 129SvJ-C57BL/6 $FAAH^{+/-}$ mice at the Scripps Research Institute, as described by Cravatt et al. (2001). Three pairs of mice were analysed at ages between 12 and 16 weeks: 680/681 (female, 16 weeks), 909/910 (male, 12 weeks) and 755/762 (female, 16 weeks). Mice were asphyxiated with CO_2 and perfused through the heart with 25 ml of 4% paraformaldehyde in phosphate-buffered saline (PBS), pH 7.4, as approved by the Queen Mary, University of London Animal Care and Use Committee and by The Home Office (UK). Moreover, the experimental procedures used were designed to minimize the number of animals used and their suffering. Brains were removed and postfixed in Bouin's fixative for at least 3 days at room temperature before embedding in paraffin wax. Coronal and saggital sections (7 or 10 μm) were cut using a Leica RM2145 microtome (Leica, Nussloch, Germany), and sets of adjacent sections were collected at 0.5 mm intervals through the brain and then mounted on glass slides coated with 2% gelatin (w/v) in chrome alum solution. Dewaxed sections were blocked with 3% normal goat serum/PBS with 0.2% Triton X-100 (PBST) and then incubated with previously characterized antibodies to a GST-fusion protein incorporating amino-acid residues 38–579 of FAAH (Egertová et al., 1998, 2000; Cravatt et al., 2001), and used here at a dilution of 1:100 in PBST. Bound antibodies were revealed using the ABC Elite kit (Vector Laboratories, Peterborough, UK). To enable comparison of FAAH expression with CB_1 cannabinoid receptor expression, series of brain sections adjacent to series that had been processed with FAAH antibodies were tested immunocytochemically with a previously characterized antiserum (2825.3) to the C-terminal tail of

mouse/rat CB_1 at a dilution of 1:1000 (see Egertová and Elphick, 2000; Egertová et al., 1998) or with antibodies affinity-purified from the CB_1-antiserum 2816.4 (see Egertová and Elphick, 2000).

Low-magnification digital images (Fig. 1) of the immunostained sections were captured using a Retiga 1300 12-bit monochrome camera (Qimaging Corp., Burnaby, B.C., Canada) linked to a Leica DMRA2 compound microscope (Leica, Nussloch, Germany). OpenLab 3.0.8 (Improvision) software was used to import images from the camera. High-magnification images (Figs. 2–9) of immunostained sections were captured using a Hamamatsu digital camera linked to a Leica DMRD microscope (Leica, Wetzlar, Germany). High Performance Image Control System (HiPic 32) software was used to import images from the camera. Digital images were processed using Adobe Photoshop software (version 5.5), removing imperfections caused by dust particles, and then labeled with reference to Paxinos and Franklin (2001).

RESULTS

General observations

Immunocytochemical analysis of FAAH expression in sections of wild type mouse brain revealed a pattern of immunostaining (Fig. 1) that was generally consistent with the distribution of FAAH mRNA expression in rat brain (Thomas et al., 1997). Moreover, to establish unequivocally the specificity of the immunostaining observed with the FAAH antibodies in the mouse brain, we analyzed brain sections from $FAAH^{-/-}$ mice alongside brain sections from their wild type littermates. Importantly, all of the immunostaining seen in $FAAH^{+/+}$ mice with FAAH antibodies was absent in $FAAH^{-/-}$ mice, as illustrated in Fig. 2A and B, respectively. These findings demonstrate that the FAAH antibodies used in this study are specific for FAAH under immunocytochemical conditions, consistent with previous analysis of $FAAH^{+/+}$ mice and $FAAH^{-/-}$ mice (Cravatt et al., 2001).

The majority of the FAAH-immunoreactivity in the mouse brain was associated with neuronal somata and their dendrites. However, in some regions of the brain FAAH-immunoreactive cells were also present in fiber tracts (white matter). This is consistent with the detection of signals for FAAH mRNA in white matter of the rat brain, as reported by Thomas et al. (1997). The morphology of the FAAH-immunoreactive cells in fiber tracts of the mouse brain indicates that these cells are oligodendrocytes (see Fig. 8C). Consistent with this hypothesis, FAAH-immunoreactivity is also evident in the myelin sheath surrounding the unstained axons of large neurons (Fig. 8C). Accordingly, myelin sheath-associated FAAH probably accounts for FAAH-immunoreactivity associated with several discrete fiber tracts in several regions of the brain (e.g. see caudate putamen, CPu in Fig. 1C).

In addition to neuronal and oligodendrocytic expression of FAAH, FAAH-immunoreactivity is also present in ependymal cells that line the ventricles of the mouse brain and this can be seen in the low magnification images of Fig. 1 but it is more clearly seen at a higher magnification in Fig. 7A. However, no CB_1-immunoreactivity is associated with the FAAH-immunoreactivity in ependymal cells. A detailed analysis of this feature of FAAH expression in the mouse brain is beyond the scope of this paper but it will be discussed in detail in a subsequent paper that will focus specifically on the role of FAAH in the ventricular epithelium (Egertová et al., unpublished observations).

Here, for the first time, we illustrate and compare the distribution of FAAH and CB_1 throughout the mouse brain based on our analysis of brains from wild type mice (BALB/c, $n=3$; 129SvJ-C57BL/6, $n=3$). Fig. 1 shows FAAH-immunostaining (A, C, E, G, I, K, M, O, Q) and CB_1-immunostaining (B, D, F, H, J, L, N, P, R) in two series of adjacent coronal sections of the brain of a single female animal (no. 680; $FAAH^{+/+}$; 129SvJ-C57BL/6). The distance between consecutive sections in each series is approximately 1 mm. The images in Fig. 1 provide an overview of the distribution of FAAH and CB_1 in the mouse brain. Moreover, below we refer to the images in Fig. 1 when discussing in detail the distribution of FAAH and CB_1 in different regions of the brain. Because of the limitations of space, it is not feasible to describe and illustrate at high magnification the distribution of FAAH and CB_1 in all regions of the mouse brain. Previously, we have described in detail and illustrated the distribution of CB_1 in the rat brain (Egertová and Elphick, 2000). Here we have focused on FAAH, and below we describe in detail and illustrate at higher magnification than the images in Fig. 1 those regions of the brain where FAAH-expressing cells are particularly abundant (Figs. 2–9). Moreover, in those brain regions where both FAAH and CB_1 are expressed at high levels we also show corresponding images of CB_1-immunoreactivity in sections adjacent to images of sections showing FAAH-immunoreactivity (Figs. 3–6).

Olfactory bulb and olfactory cortex

Inspection of Fig. 1A and B reveals that intense FAAH-immunoreactivity is evident in the olfactory bulb (OB; Fig. 1A) compared with relatively low levels of CB_1 expression (Fig. 1B). More specifically and most noteworthy, FAAH is particularly abundant in fibers of the olfactory nerve (ON) and in the olfactory glomeruli (Gl) (Fig. 2A). FAAH-immunoreactivity is also evident in the somata and dendrites of mitral cells (Mi; Fig. 2A), consistent with previous analysis of rat brain (Tsou et al., 1998). Relatively weak FAAH-immunoreactivity can also be seen in the granule cell layer (GrO) of the olfactory bulb (Fig. 2A).

FAAH-immunoreactive neuronal somata are evident in the majority of the cortical olfactory regions that receive direct input from the olfactory bulbs. These include the anterior olfactory nucleus (AON; Figs. 1A, 3A), the piriform cortex (Pir; Figs. 1C, E, G, I; 3C), the tenia tecta (DTT; Figs. 1C; 3E) and the indusium griseum (IG; Fig. 1C, E), and in all of these regions FAAH-immunoreactive neuronal somata are surrounded by a complementary network of CB_1-immunoreactive fibers (Figs. 1B, D, F, H, J; 3B, D, F). FAAH-immunoreactive neurons are not, however, evident in the olfactory tubercle, a region of the olfactory cortex that contains a fine meshwork of CB_1-immunoreactive fibers in both mouse (not shown) and rat (Egertová and Elphick, 2000).

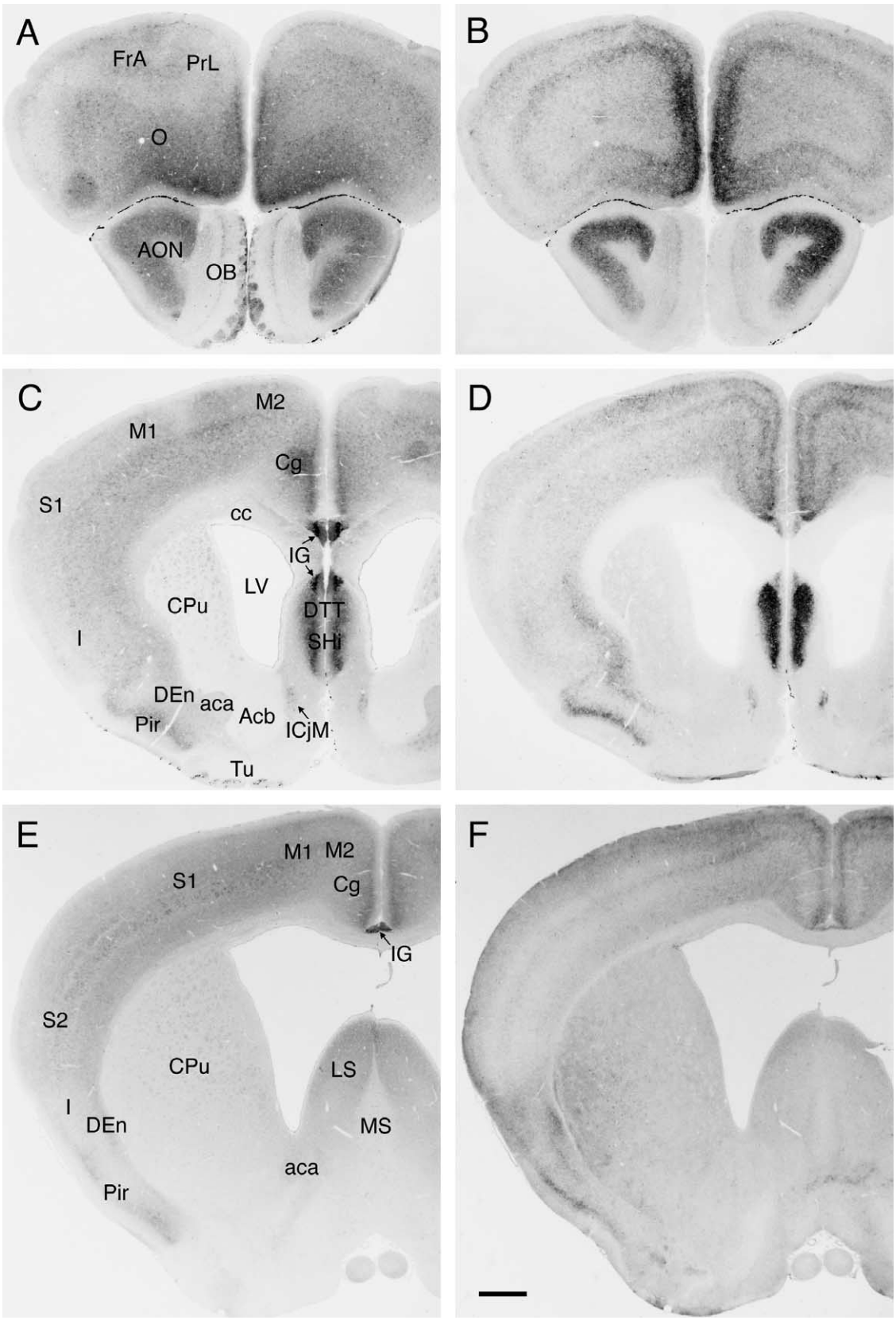

Fig. 1. The distribution of FAAH (left column; A, C, E, G, I, K, M, O, Q) and CB_1 (right column; B, D, F, H, J, L, N, P, R) in a series of adjacent coronal sections of the mouse brain as revealed by immunocytochemistry. Scale bar=0.5 mm.

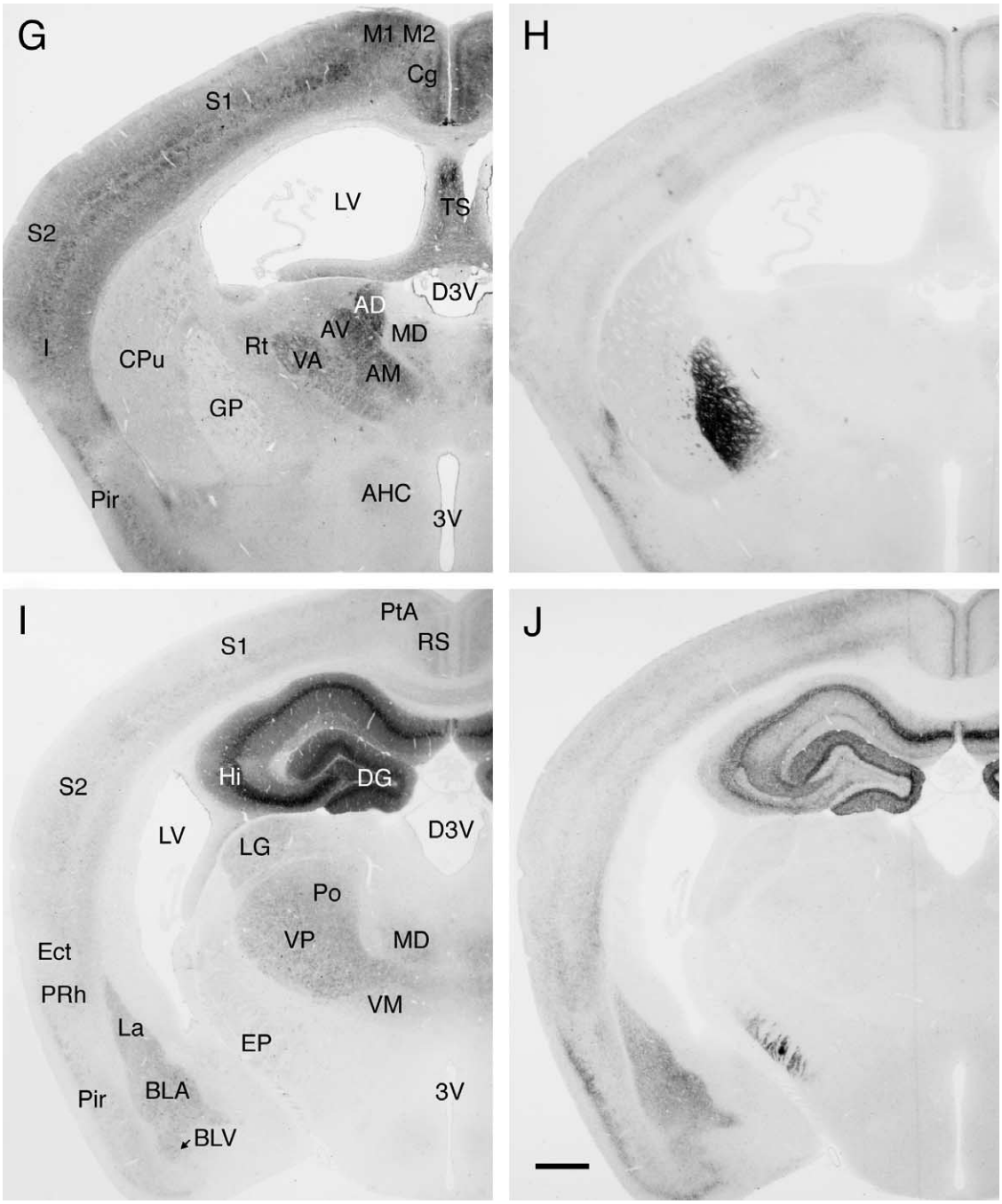

Fig. 1. *(Continued).*

Septum, amygdala and hippocampal formation

Neuronal FAAH-immunoreactivity was detected in the lateral septum (LS; Fig. 1E) and the triangular septal nucleus (TS; Fig. 1G) with associated low-level expression of CB_1 (Fig. 1F, H). FAAH-immunoreactive neuronal somata are also present throughout the basolateral complex of the amygdala, which includes the lateral (La), basolateral (BLA, BLV) and basomedial (BMP) nuclei (Figs. 1I; 4A). In all of these nuclei the FAAH-immunoreactive neuronal somata are surrounded by CB_1- immunoreactive fibers (Figs. 1J; 4B).

Consistent with previous analysis of the rat brain (Egertová et al., 1998), FAAH-immunoreactivity was detected in the somata and dendrites of pyramidal cells throughout the hippocampus (Figs. 1I, K; 5A, E). In addition, however, FAAH-immunoreactivity is also evident in the somata of dentate gyrus granule cells (DG; Figs. 1I, K; GrDG; 5A, C). This is of particular interest because, although FAAH mRNA has been detected in these cells in

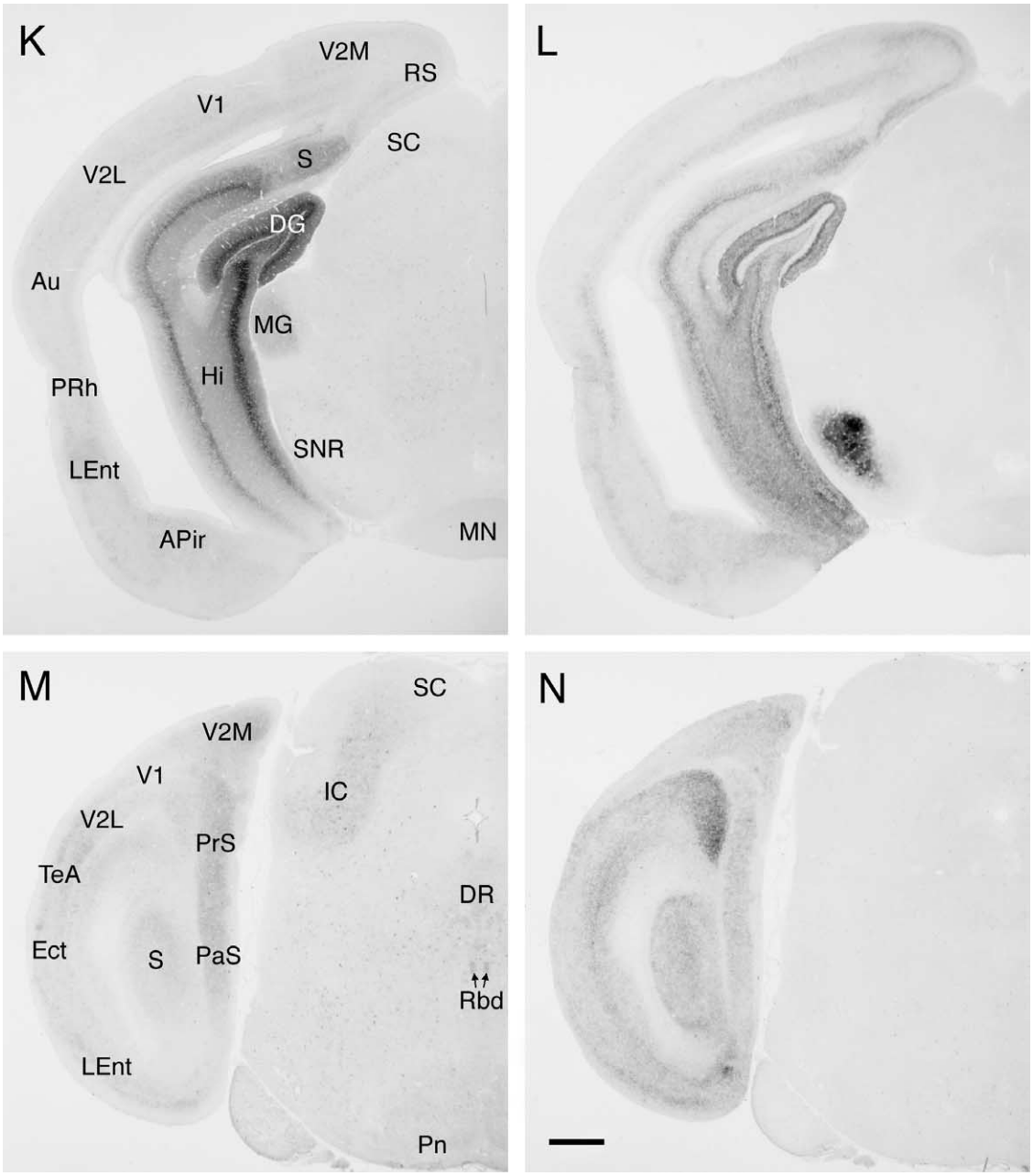

Fig. 1. *(Continued).*

the rat brain (Thomas et al., 1997), FAAH-immunoreactivity is not evident in granule cells of the rat dentate gyrus (Tsou et al., 1998; our unpublished observations). CB_1-immunoreactivity was detected in a dense meshwork of fibers surrounding both hippocampal pyramidal cells (Figs. 1J, K; 5B, F) and granule cells of the dentate gyrus (Figs. 1J, K; 5B, D), respectively, as in the rat brain (Egertová and Elphick, 2000).

Cerebral cortex and cerebellar cortex

FAAH-immunoreactive neuronal somata are present throughout transitional (e.g. orbital [O] cortex; Figs. 1A; 6C) and neocortical regions (e.g. primary somatosensory [S1] cortex; Figs. 1C, E, G, I; 6A) of the cerebral cortex, and are surrounded by CB_1-immunoreactive fibers (Figs. 1D, F; 6B, D). FAAH-immunoreactive neuronal somata are evident in all layers except layer I, the most striking of which are large cells present in layer V (Fig. 6A). CB_1-immunoreactivity is present in a network of fibers in all layers but the density of these fibers is highest in layers II and III, the outer region of layer V and throughout layer VI with layers I, IV and V (inner) showing much sparser fiber staining (Fig. 6B).

Consistent with previous analysis of the rat cerebellar cortex (Egertová et al., 1998), FAAH-immunoreactivity was

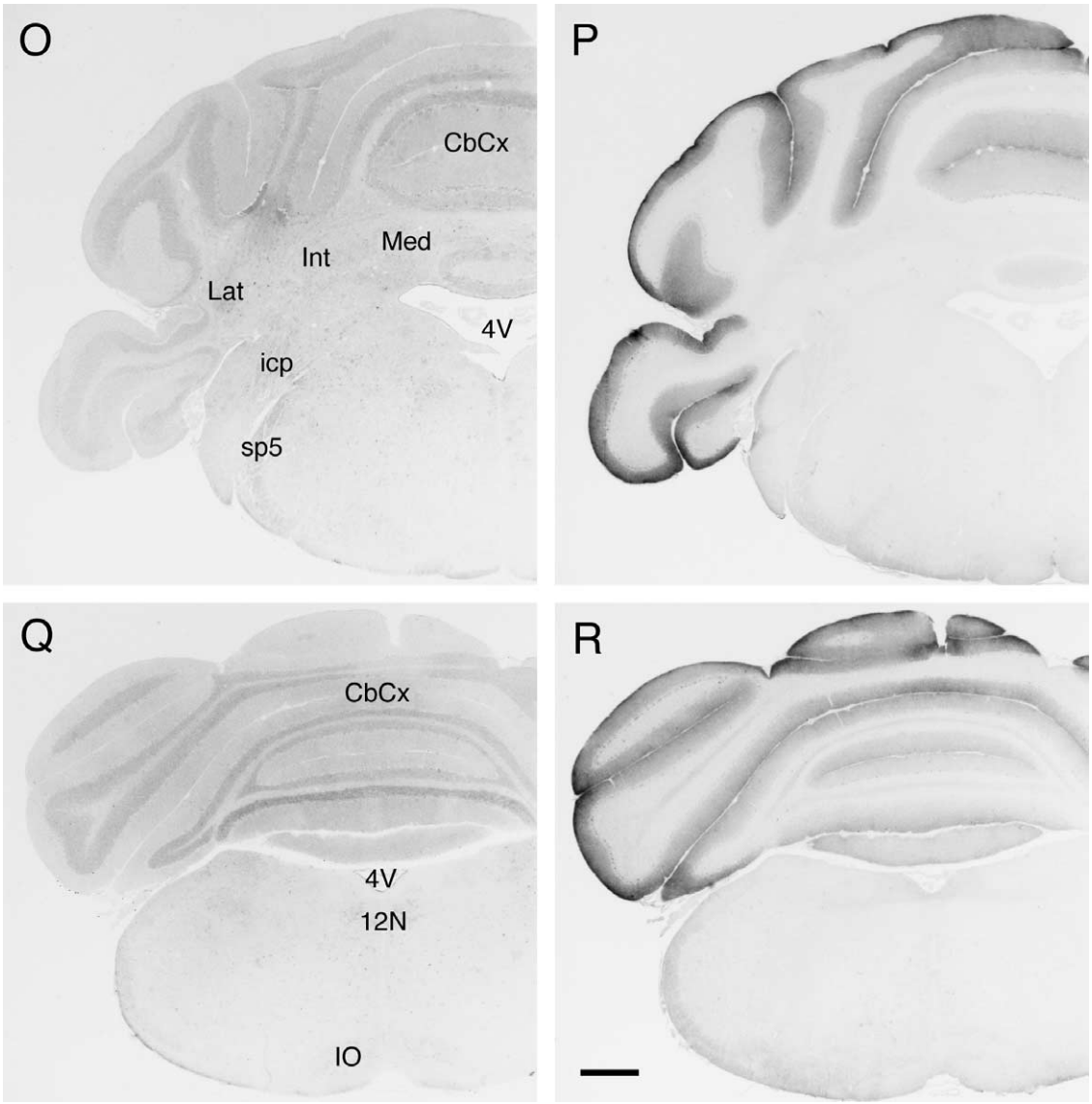

Fig. 1. *(Continued).*

detected in the somata of Purkinje cells (PCL; Fig. 6E). However, the dendritic branches of the Purkinje cells contained little or no FAAH-immunoreactivity. FAAH-immunoreactivity was also evident in the somata of granule cells (GrL), although the intensity of staining is quite weak (Fig. 6E). This is consistent with the detection of FAAH mRNA in rat cerebellar granule cells (Thomas et al., 1997), although in the rat FAAH-immunoreactivity is not evident in these cells (Egertová et al., 1998; Tsou et al., 1998). As in rat brain, CB_1-immunoreactivity was detected in the axon terminals of basket cells surrounding Purkinje cell somata and in a dense meshwork of fibers in the molecular layer (ML) surrounding Purkinje cell dendrites (Fig. 6F). CB_1-immunoreactivity in the molecular layer is largely associated with the parallel fibers of granule cells, consistent with CB_1 mRNA expression in granule-cell somata (Matsuda et al., 1993).

Thalamus

FAAH-immunoreactivity was detected in neuronal somata in the majority of thalamic nuclei, including the anterodorsal (AD; Figs. 1G; 7A), the anteroventral (AV; Figs. 1G; 7A), the anteromedial (AM, Figs. 1G; 7A), the ventroanterior (VA; Figs. 1G; 7A), the paratenial (PT; Fig. 7A), the mediodorsal (MD; Figs. 1G, I; 7A, B), the reticulothalamic (Rt; Figs. 1G; 7B), the ventrolateral (VL; Fig. 7B), the ventroposterior (VP; Figs. 1I; 7B, C), the ventromedial (VM; Figs. 1I; 7B), the posterior (Po; Figs. 1I; 7C), the lateral geniculate (LG; Fig. 7C) and the medial geniculate (MG; 1K). Importantly, however, little or no CB_1-immunoreactivity was detected in the thalamus (Fig. 1H, J). This is consistent with the findings of Herkenham et al. (1991) who detected only low concentrations of cannabinoid-binding sites in thalamic nuclei

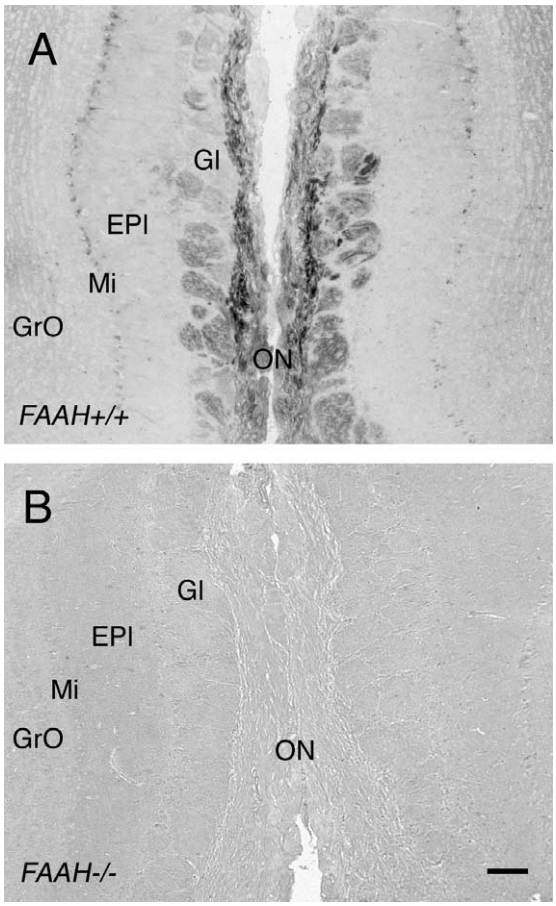

Fig. 2. Localization of FAAH in the olfactory bulb of wild type ($FAAH^{+/+}$) mouse brain (A) and absence of FAAH-immunoreactivity in the olfactory bulb of a $FAAH^{-/-}$ mouse (B). (A) FAAH-immunoreactivity is present in the axons of olfactory receptor neurons in the olfactory nerve (ON) and in the glomerular layer (Gl). FAAH-immunoreactivity is also present in the somata of mitral cells (Mi) and in the granule cell layer of the olfactory bulb (GrO). (B) Shows absence of immunoreactivity with FAAH antibodies in the olfactory bulb of $FAAH^{-/-}$-mice, demonstrating the specificity of FAAH-immunoreactivity observed in the olfactory bulbs and in other brain regions. Scale bar=100 μm.

of the rat brain. Thus, the thalamus represents a region of the brain where FAAH-immunoreactive neurons are particularly abundant but with few or no associated CB_1-expressing fibers.

Mid-brain

FAAH-immunoreactive neurons are present in the inferior colliculus (IC; Figs. 1M; 8A), the superior colliculus (not shown), the rhabdoid nucleus (Rbd; Figs. 1M; 8B), several mesencephalic raphe nuclei (MnR, DR; Figs. 1M; 8B) and the mesencephalic trigeminal nucleus (Me5; Fig. 8C). Little or no CB_1-immunoreactivity is evident in these regions of the brain (Fig. 1L, N). Conversely, FAAH-immunoreactive neurons were not evident, however, in the substantia nigra pars reticulata (SNR; Fig. 1K), a region of the mid-brain that contains a very high concentration of CB_1-immunoreactivity in both mouse (Fig. 1L) and rat (Egertová and Elphick, 2000).

In the mid-brain, the expression of FAAH by oligodendrocytes is particularly striking. For example, in Fig. 8B FAAH-immunoreactive oligodendrocytes associated with fiber tracts (mlf; xscp) are abundant and more intensely stained than the FAAH-immunoreactive neurons in the raphe nuclei. Moreover, Fig. 8C shows a clear example of a FAAH-immunoreactive oligodendrocyte with a process that is continguous with FAAH-immunoreactive myelin sheath surrounding unstained axons in the mesencephalic trigeminal tract (me5).

Hind-brain

In the hind brain, in addition to FAAH-immunoreactivity associated with the cerebellar cortex (see above), FAAH-immunoreactive neurons are present in the hypoglossal nucleus (12N; Figs. 1Q; 9A) and the inferior olive (IO; Figs. 1Q; 9B), but little or no CB_1-immunoreactivity was evident in these nuclei (Fig. 1R). FAAH-immunoreactivity was also detected in the somata of neurons in the cerebellar nuclei (Figs. 1O; 9C), which receive synaptic input from Purkinje cell axons. In white matter surrounding the cerebellar nuclei, FAAH-immunoreactive oligodendrocytes are particularly abundant (Fig. 9C) and Fig. 9C shows how much more intensely stained these glial cells are compared to neighbouring neurons. The cerebellar nuclei are, however, void of CB_1-immunoreactivity (Fig. 1P), consistent with the absence of cannabinoid-binding sites in these nuclei in the rat brain (Herkenham et al., 1991).

DISCUSSION

Here we report the first detailed analysis of the distribution of FAAH in the mouse brain, using $FAAH^{-/-}$ mice as negative controls to provide an unequivocal determination of the specificity of immunostaining in wild type animals. The majority of FAAH in the mouse brain is associated with neurons and it is the presence of FAAH in neurons that is probably most directly relevant to endocannabinoid signaling, as discussed below. An interesting feature of neuronal FAAH-immunostaining in several regions of the brain was that FAAH-immunoreactivity appears not to be confined to neuronal somata but also extends into surrounding areas of neural tissue. This is most clearly seen in the hippocampal formation where, although the highest concentration of FAAH-immunoreactivity is clearly located in the somata of hippocampal pyramidal cells and granule cells of the dentate gyrus, there is also widespread immunostaining in adjacent layers that contain their axons and dendrites (Fig. 5A, C, E). The diffuse and homogeneous nature of this staining suggests that it is not compartmentalized within neuronal processes but is located extracellularly. One possibility is that this putative extracellular FAAH-immunoreactivity is an artifact of tissue preparation resulting from lysis of FAAH-expressing neuronal somata. An alternative and more intriguing explanation, however, is that it reflects active secretion of FAAH (either in soluble or vesicle-associated form) into the surrounding extracellular medium by FAAH-expressing neurons.

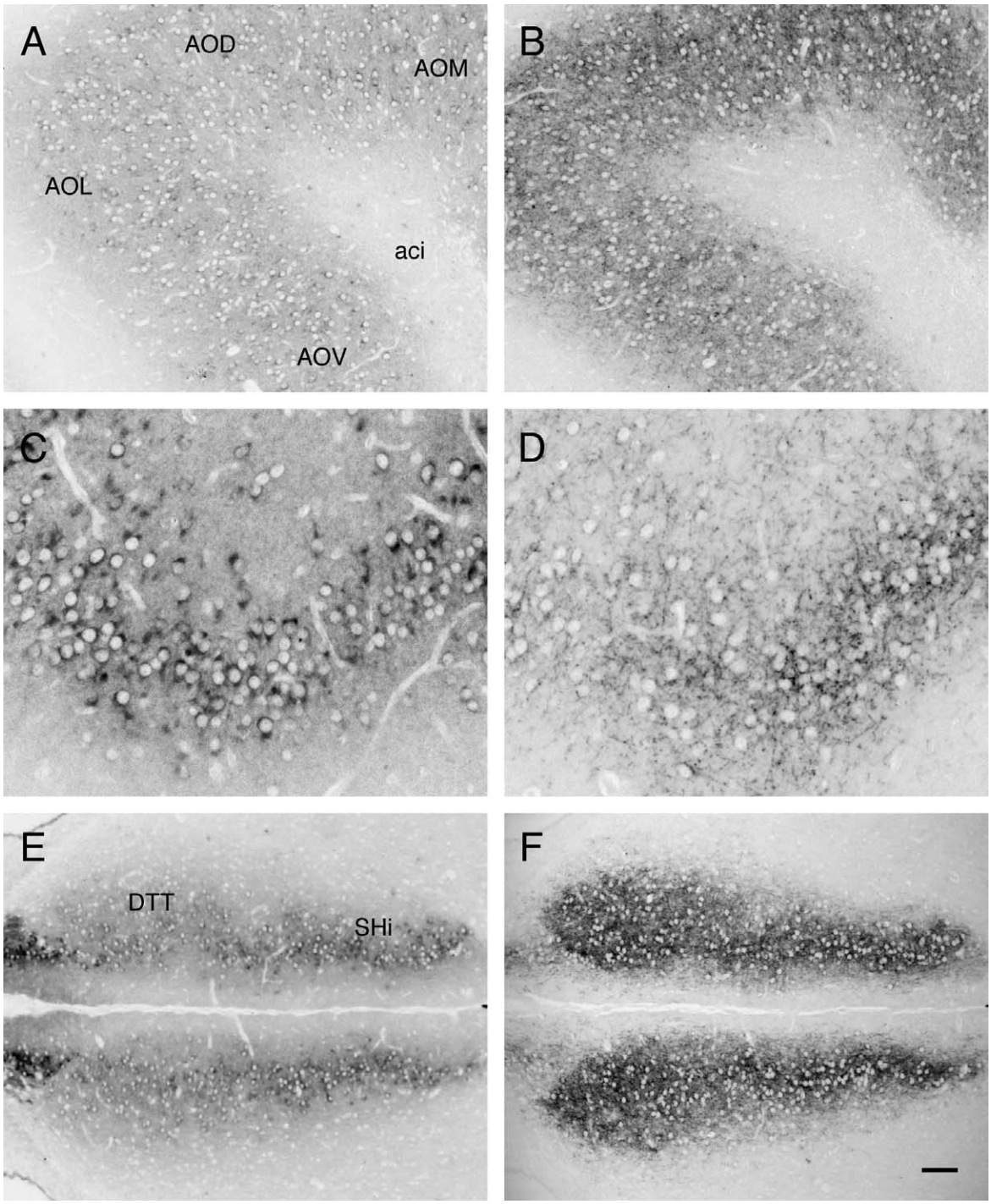

Fig. 3. Localization of FAAH-immunoreactivity (A, C, E) and CB_1-immunoreactivity (B, D, F) in adjacent sections of regions of the olfactory cortex: anterior olfactory nucleus (A, B), piriform cortex (C, D) and tenia tecta (E, F). In all three regions FAAH-immunoreactive neuronal somata (A, C, E) are surrounded by CB_1-immunoreactive fibers (B, D, F). Scale bar=50 μm in A and B, 25 μm in C and D, 67 μm in E and F.

Probably the most striking and intensely stained FAAH-immunoreactive neurons of the entire mouse brain were to be found in the mesencephalic trigeminal nucleus (Me5), as shown in Fig. 8C. These neurons are of particular interest because they are functionally homologous to sensory neurons of the dorsal root ganglia and they are the only primary sensory neurons with cell bodies located within the central nervous system (Holstege et al., 1995).

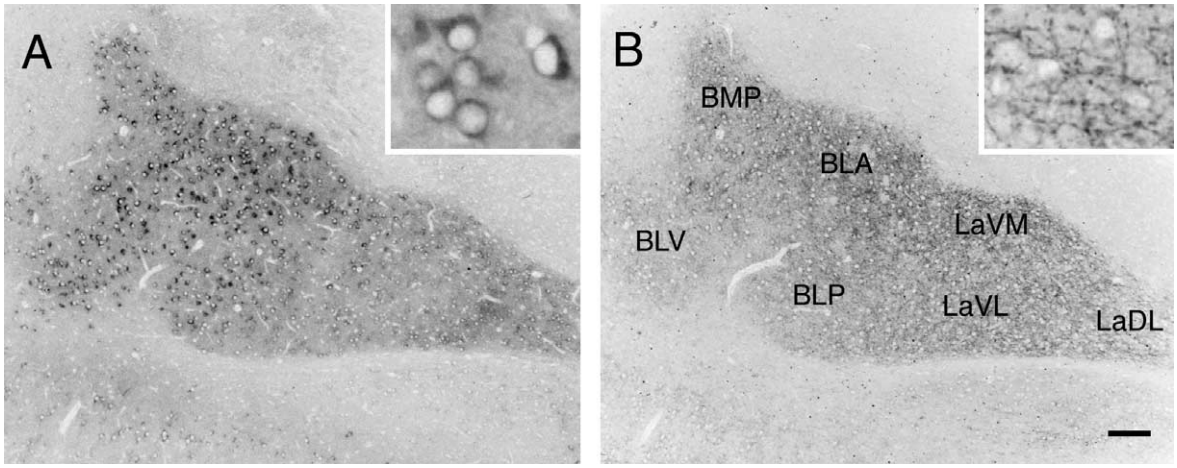

Fig. 4. Localization of FAAH immunoreactivity (A) and CB immunoreactivity (B) in the basolateral complex of the amygdala showing that FAAH-immunoreactive neuronal somata are surrounded by CB_1-immunoreactive fibers. A and B show FAAH (A) and CB_1 (B) immunoreactivity in low-magnification images of adjacent sections of the amygdala. The inset of A shows detail of FAAH-immunoreactive neuronal somata in BMP whilst the inset of B shows detail of CB_1-immunoreactive fibers in LaVM. Scale bar=100 μm in A and B, and to 16 μm in the insets of A and B.

Physiologically these neurons are involved in mediating jaw opening and closing reflexes and it will therefore be of specific interest to investigate the functional significance of FAAH expression in their somata.

In addition to neuronal FAAH expression, FAAH is also expressed by oligodendrocytes and ventricular ependymal cells of the mouse brain. The functional significance of FAAH expression in these non-neuronal cells is not yet known and therefore this study represents the starting point for a new aspect of FAAH research. The association of FAAH with oligodendrocytes in fiber tracts is, however, of particular interest with respect to a recent study showing that FAAH activity in the striatum is reduced in a rat model of Parkinson's disease in which inputs to the striatum from the substantia nigra are disrupted (Gubellini et al., 2002). We speculate that the loss of neuronal inputs to the striatum from the substantia nigra may also lead to loss of associated FAAH-expressing oligodendrocytes, which could account for the reduced levels of striatal FAAH in rats with experimental Parkinsonism.

To address the main objective of this study and assess the potential role of FAAH in endocannabinoid signaling, we have compared the distribution of FAAH with that of the CB_1 cannabinoid receptor throughout the mouse brain. We have identified: (1) regions of the brain where FAAH is expressed with little or no associated CB_1; (2) regions of the brain where there is expression of both FAAH and CB_1; and (3) regions of the brain where CB_1 is expressed with little or no associated FAAH. Below we will consider the functional significance of these findings and, in particular, the potential role of FAAH in regulation of the spatiotemporal dynamics of retrograde signaling by endocannabinoids.

Regions of the brain where FAAH-expressing neurons are present but accompanied by few or no CB_1-expressing fibers include the thalamus, mid-brain and hind brain. In some brain regions (e.g. hypoglossal nucleus, median raphe nucleus), the absence of CB_1-immunoreactivity may simply reflect insensitivity of the immunocytochemical methods used here because there is evidence for the presence of low-level cannabinoid receptor expression from radioligand binding studies (Herkenham et al., 1991). However, there clearly are some regions of the brain (e.g. thalamic nuclei, mesencephalic trigeminal nuclei, cerebellar nuclei) where FAAH-immunoreactive neurons are widespread but in the absence of associated CB_1 expression. In regions of the brain such as these, the role of FAAH is likely to be unrelated to CB_1-dependent endocannabinoid signaling mechanisms. Intriguingly, it is possible that in these regions of the brain, FAAH participates in regulation of signaling mediated by a novel G protein coupled anandamide receptor discovered recently in the brains of $CB_1^{-/-}$ mice (Breivogel et al., 2001). Alternatively, in these regions of the brain FAAH may be involved in inactivation of fatty acid amide signaling molecules that exert their effects via non-cannabinoid receptors. For example, there is evidence that oleamide exerts effects in the thalamus via allosteric interaction with the serotonin 5-HT_7 receptor (Thomas et al., 1999) and the presence of FAAH in thalamic neurons may regulate the actions of this sleep-inducing lipid.

More typically, however, FAAH and CB_1 are anatomically associated, with FAAH-immunoreactive neuronal somata surrounded by CB_1-immunoreactive fibers, as reported previously in the rat cerebellar cortex, hippocampus and neocortex (Egertová et al., 1998). Based on this anatomical relationship between FAAH and CB_1 expression, we predicted that endocannabinoids may act as retrograde signaling molecules at synapses in the brain (Egertová et al., 1998; Elphick and Egertová, 2001) and experimental studies on the hippocampus and cerebellar cortex have proved that this hypothesis was correct (Kreitzer and Regehr, 2001a,b; Maejima et al., 2001a,b; Ohno-Shosaku et al., 2001; Wilson and Nicoll, 2001; Wilson et al., 2001). Therefore, it seems likely that endocannabinoids may also act as retrograde messengers at synapses in the many

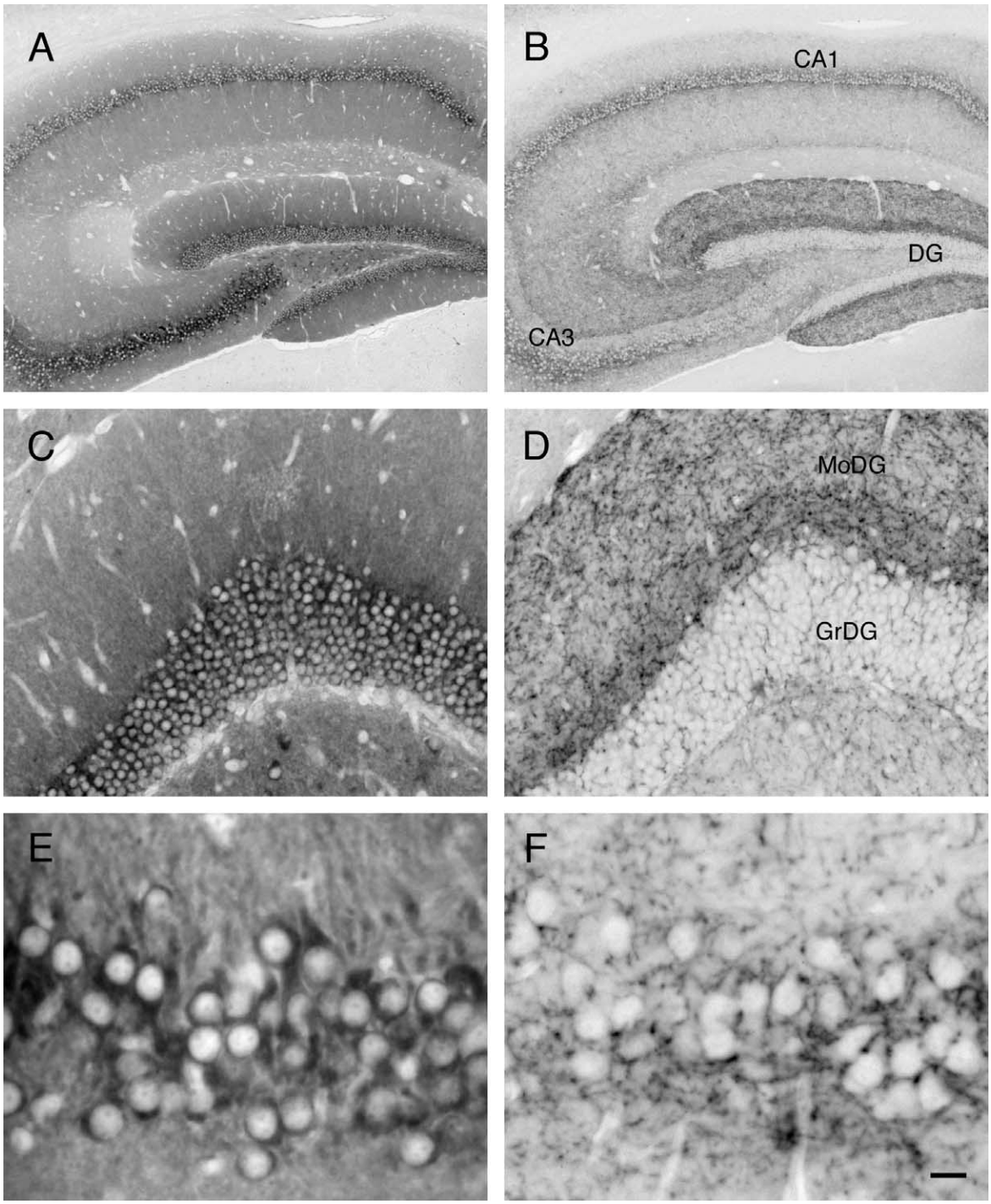

Fig. 5. Localization of FAAH-immunoreactivity (A, C, E) and CB_1-immunoreactivity (B, D, F) in the hippocampal formation. A and B show FAAH (A) and CB_1 (B) immunoreactivity in low-magnification images of adjacent sections of the hippocampus (CA1–CA3) and the dentate gyrus (DG). (C) Detail of FAAH-immunoreactivity in the dentate gyrus showing that whilst FAAH is concentrated in the granule cell layer, diffuse and homogeneous immunoreactivity is also evident throughout the molecular layer, which may reflect active secretion of the enzyme (see discussion). (D) Detail of CB_1 immunoreactivity in the dentate gyrus showing that immunoreactive fibers are present surrounding the unstained somata of granule cells (GrDG) and throughout the molecular layer (MoDG) where the dendrites of granule cells arborize. (E) Detail of FAAH-immunoreactivity in the hippocampus showing that FAAH is concentrated in the somata of pyramidal cells but is also present in adjacent layers. (F) Detail of CB_1-immunoreactivity in the pyramidal cell layer of the hippocampus showing that immunoreactive fibers are present surrounding the unstained somata of pyramidal cells. Scale bar=111 μm in A and B, 25 μm in C and D and 10 μm in E and F.

regions of the brain that we describe here where "complementary" expression of FAAH and CB_1 occurs, which include the olfactory cortex, amygdala, dentate gyrus, transitional cortex and neocortex. Moreover, it is important to

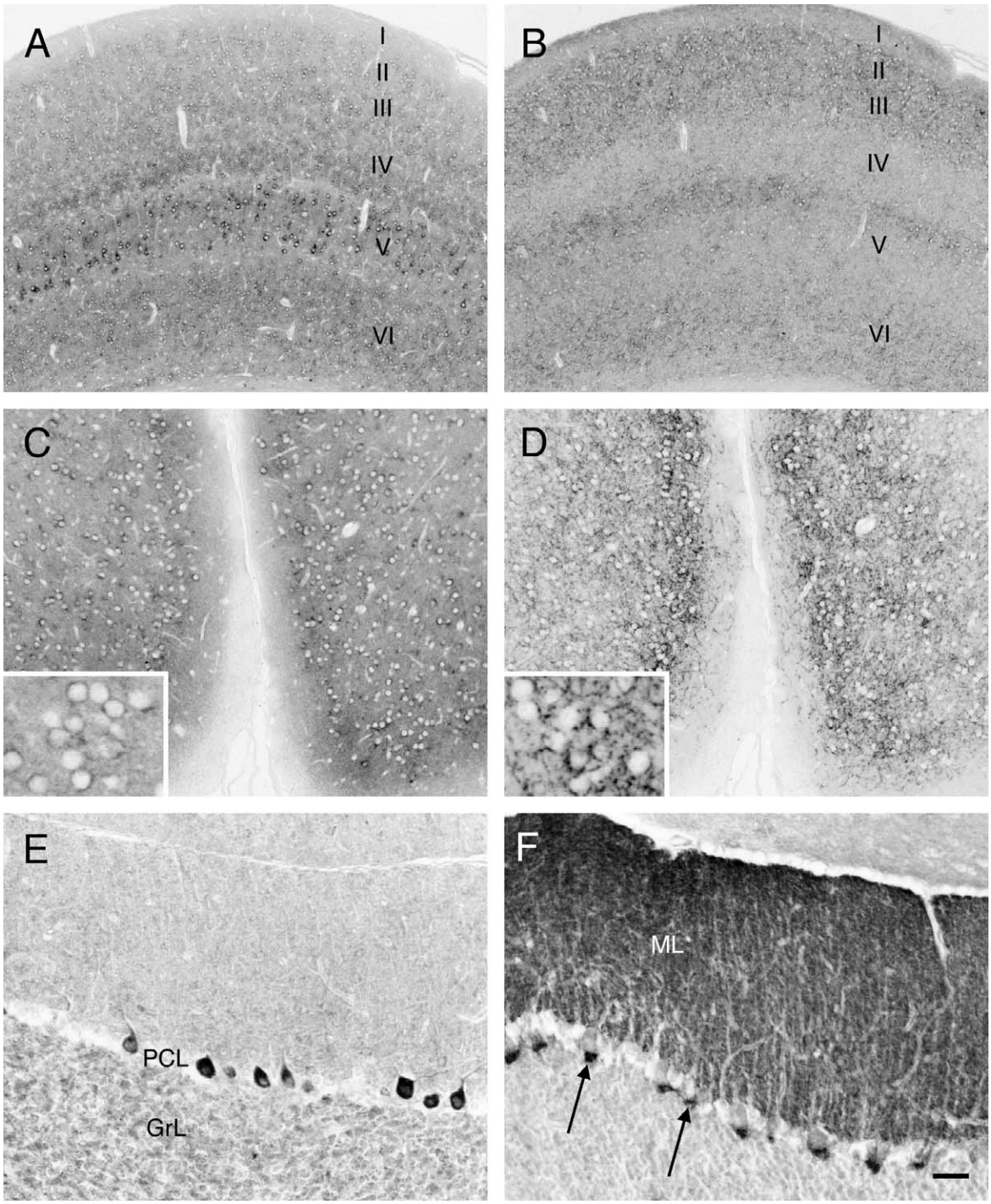

Fig. 6. Localization of FAAH-immunoreactivity (A, C, E) and CB_1-immunoreactivity (B, D, F) in cerebral cortex and cerebellar cortex. A and B show adjacent sections of primary somatosensory cortex, as a representative region of neocortex. FAAH-immunoreactive neuronal somata are present in all layers of the cortex except layer I but large cells in layer V are more intensely stained than cells in other layers. CB_1- immunoreactive fibers are present in all layers of the neocortex surrounding unstained neuronal somata. However, the density of CB_1-immunoreactive fibers is highest in layers II, III, V-outer and VI whilst layers I, IV and V-inner contain fewer immunoreactive fibers. C and D show adjacent sections of medial orbital cortex, as a representative region of transitional cortex. Note the complementary pattern of FAAH and CB_1 expression with CB_1-immunoreactive fibers (inset of D) surrounding FAAH-immunoreactive neuronal somata (inset of C). (E) Purkinje cells in the Purkinje cell layer (PCL) of the cerebellar cortex are strongly FAAH-immunoreactive whilst cells of the granule cell layer (GrL) display weak FAAH-immunoreactivity. (F) CB_1-immunoreactivity in the cerebellar cortex is complementary to FAAH, with intense immunostaining in fibers of the molecular layer (ML) and in the axon terminals of basket cells (arrows). Scale bar=100 μm in A and B, 50 μm in C and D, 15 μm in the insets of C and D, and 25 μm in E and F.

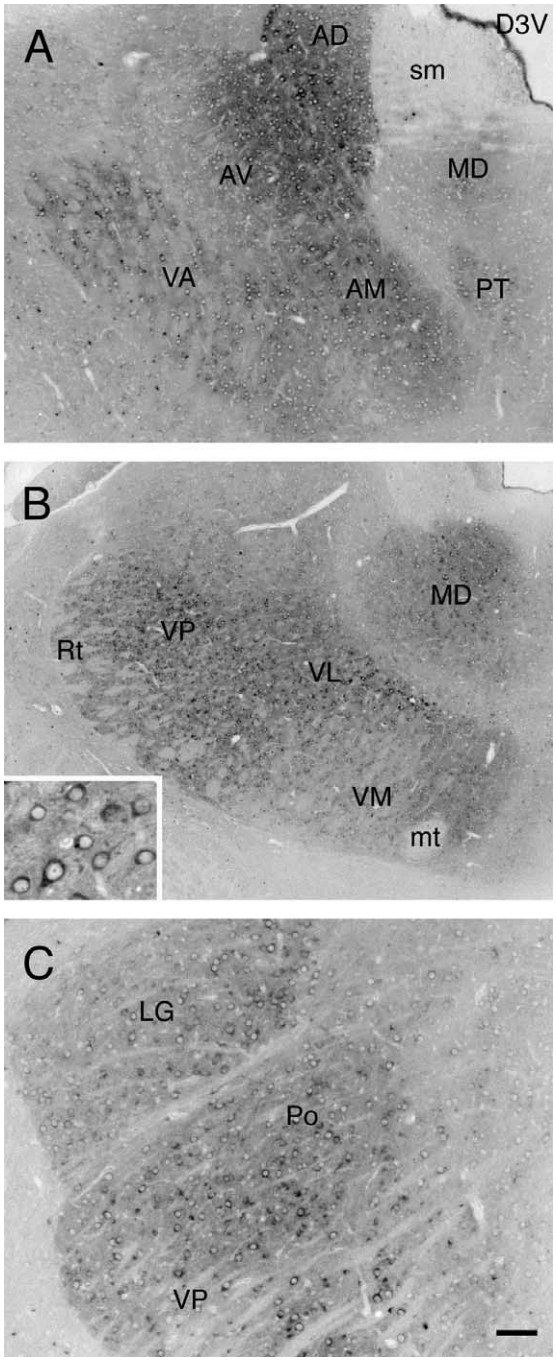

Fig. 7. Localization of FAAH-immunoreactivity in thalamic nuclei. (A) FAAH- immunoreactive neuronal somata in the anterodorsal (AD), the anteroventral (AV), the anteromedial (AM), paratenial (PT), the mediodorsal (MD) and reticulothalamic (Rt) nuclei. Note also the immunostaining in ependymal cells lining the dorsal third ventricle (D3V) and the absence of immunostaining in the stria medullaris (sm). (B) FAAH-immunoreactive neuronal somata in the mediodorsal (MD), the reticulothalamic (Rt), the ventrolateral (VL), the ventroposterior (VP) and the ventromedial (VM) nuclei. The inset shows FAAH-immunoreactive neuronal somata in the ventroposterior thalamic nucleus at high magnification. (C) FAAH-immunoreactive neuronal somata in the VP, the posterior (Po) and the lateral geniculate (LG) nuclei. Scale bar=100 μm in A, 154 μm in B, 25 μm in the inset of B and 56 μm in C.

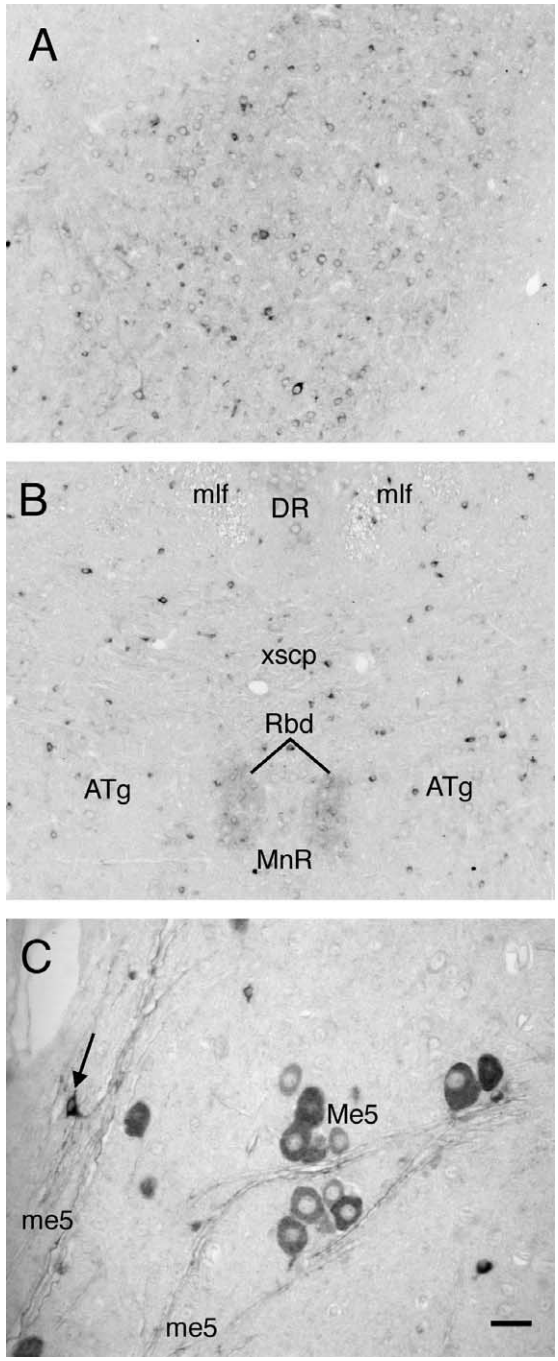

Fig. 8. FAAH-immunoreactivity in mid-brain regions. (A) FAAH-immunoreactive neurons in the inferior colliculus. (B) FAAH-immunoreactive neurons in the rhabdoid nuclei (Rbd) and the median (MnR) and dorsal (DR) raphe nuclei. Note the intensely stained cells (oligodendrocytes) in fiber tracts of the decussation of the superior cerebellar peduncle (xscp) and the medial longitudinal fasciculus (mlf). (C) FAAH-immunoreactive neuronal somata in a saggital section through the mesencephalic trigeminal nucleus (Me5). Note also the strongly stained oligodendrocyte (arrow) with a process projecting into a fiber bundle of the mesencephalic trigeminal tract (me5). The fibrous staining in me5 appears to be localized in the myelin sheath surrounding the unstained axons of Me5 neurons, consistent with FAAH expression by oligodendrocytes. Scale bar=50 μm in A and B and to 25 μm in C.

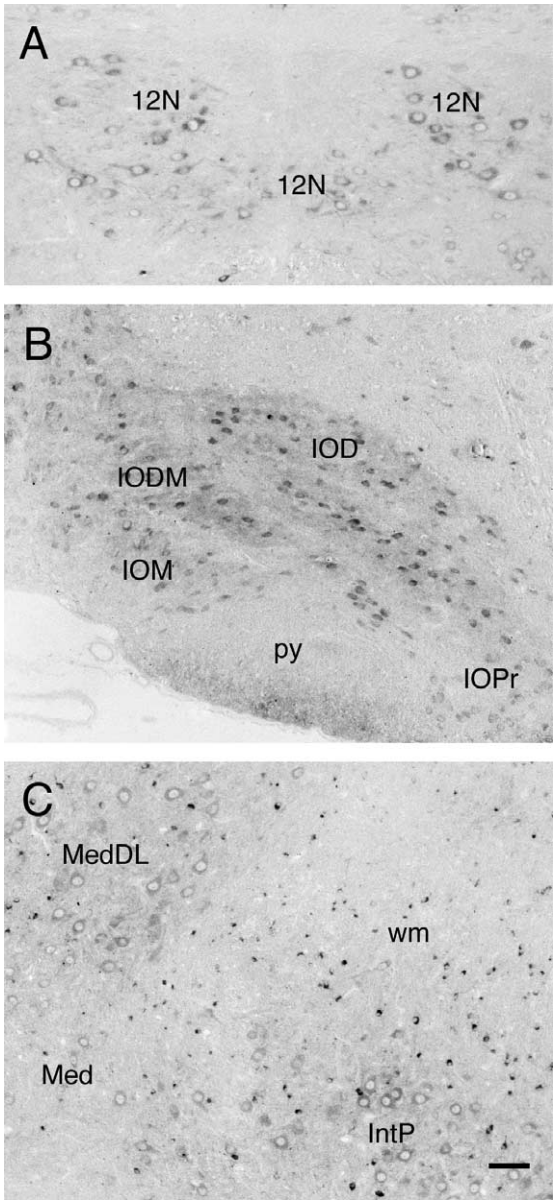

Fig. 9. FAAH-immunoreactivity in hind-brain regions. (A) FAAH-immunoreactive neurons in the hypoglossal nucleus (12N). (B) FAAH-immunoreactive neurons in the dorsomedial cell group (IODM), the medial nucleus (IOM), the dorsal nucleus (IOD) and the principal nucleus (IOPr) of the inferior olive, dorsal to the pyramidal tract (py). (C) FAAH-immunoreactive neurons in the posterior interposed cerebellar nucleus (IntP), the medial cerebellar nucleus (Med) and the dorsolateral protruberance of the medial cerebellar nucleus (MedDL). Note also the intensely stained small cells (oligodendrocytes) in the cerebellar nuclei and surrounding white matter (wm). Scale bar=50 μm in A, B and C.

consider how FAAH may influence the dynamics of retrograde signaling by endocannabinoids at synapses.

In analyzing the spatial dynamics of retrograde signaling by endocannabinoids in the hippocampus, Wilson and Nicoll (2001) conclude that their effects are restricted to a sphere with a diameter of about 40 μm surrounding the pyramidal cell to which a depolarizing stimulus has been applied. Moreover, Carlson et al. (2002) have found that release of endocannabinoids by a pyramidal cell causes a normally ineffective train of excitatory post-synaptic currents to induce long-term potentiation (LTP) in that cell but not in neighbouring cells. Because FAAH is located in the somata and dendrites of hippocampal pyramidal cells, the activity of this enzyme is likely to be a key determinant of the distance over which endocannabinoids diffuse from a cellular site of synthesis before being inactivated. Thus, the presence of FAAH in pyramidal cell somata may confine endocannabinoid-facilitated LTP to cells in which endocannabinoid biosynthesis has been triggered. Moreover, FAAH probably exerts such a regulatory role in the spatial dynamics of retrograde signaling by endocannabinoids not only in the hippocampus but also in the many regions of the brain that we describe here where FAAH is located in neuronal somata and/or dendrites surrounded by CB_1-immunoreactive fibers. For example, a complementary pattern of FAAH and CB_1 expression like that seen in the hippocampus is also evident in the cortex of the forebrain and in subcortical regions such as the amygdala. Accordingly, several recent studies indicate that endocannabinoids also act as retrograde synaptic signaling molecules in these regions of the forebrain (Katona et al., 2001; Trettel and Levine, 2002).

FAAH is likely to influence not only the spatial dynamics of cannabinoid signaling but also the temporal dynamics. Evidence for such a role is apparent in the cerebellar cortex where endocannabinoids mediate retrograde suppression of both excitatory and inhibitory synapses onto Purkinje cells (Kreitzer and Regehr, 2001a,b; Maejima et al., 2001b). Here FAAH is located in Purkinje cell somata, whilst CB_1 is located on the presynaptic terminals of granule cells (glutamatergic parallel fibers), basket cells (GABAergic) and probably also climbing fibers (glutamatergic). Depolarization of Purkinje cells causes transient endocannabinoid-mediated inhibition of excitatory inputs from parallel fibers and climbing fibers with maximal inhibition occurring after approximately 5 s, followed by a gradual restoration of basal excitatory input within 50 s (Kreitzer and Regehr, 2001a). Because FAAH is located in the somato-dendritic compartment of Purkinje cells, the duration of the inhibitory action of Purkinje cell-derived endocannabinoids is likely to be largely influenced by uptake and FAAH-mediated inactivation of endocannabinoids in Purkinje cells.

Importantly, the dynamics of retrograde endocannabinoid signaling may be influenced not only by the presence of FAAH in the somata of neurons that are postsynaptic to CB_1-expressing fibers but also by the expression of FAAH by other nearby cells. For example, in the cerebellar cortex the presence of FAAH in the somata of granule cells may influence the dynamics of retrograde signaling from the principal cells (Purkinje cells) to the presynaptic terminals of parallel fibers, climbing fibers and basket cells. Conversely, in the olfactory bulb, retrograde endocannabinoid signaling may operate at the synapses between CB_1-immunoreactive projection neurons from the anterior olfactory nucleus and FAAH-immunoreactive granule cells.

However, the dynamics of cannabinoid signaling may also be influenced by the presence of FAAH in principal cells of the olfactory bulb (mitral cells). Moreover, in mouse olfactory bulbs FAAH is also present in fibers of the olfactory nerves that project into the olfactory bulb glomeruli where they form synapses with the glomerular dendrites of mitral cells. This is of particular interest because it is the first example, to the best of our knowledge, where FAAH is targeted to the axonal compartment of neurons because in all other regions of the mouse and rat brain it is targeted to the somato-dendritic compartment of neurons. It also provides a unique example of a synapse where FAAH is located both presynaptically (olfactory-receptor neuron terminals) and postsynaptically (mitral cells). The functional significance of this complex pattern of expression is not yet clear, but it may reflect the unusual synaptic organization of olfactory glomeruli (see Shepherd and Greer, 1998).

The distribution of CB_1 in the brain, although strikingly complementary with FAAH in many regions of the forebrain and in the cerebellar cortex, is not always associated with FAAH-expressing neurons. For example, there is a population of striatal GABAergic medium-spiny projection neurons that target the CB_1 receptor to their axonal terminals in globus pallidus (GP), entopeduncular nucleus (EP) and substantia nigra pars reticulata (SNR). The density of CB_1 receptors in these output nuclei is particularly high (Fig. 1H, J, L), whilst FAAH-expressing neurons are sparse or absent (Fig. 1G, I, K). This may in part simply reflect the neuroarchitecture of these brain regions, but nevertheless it is of interest to consider the mechanisms of cannabinoid signaling at striatal output synapses. A recent study by Wallmichrath and Szabo (2002) demonstrated that cannabinoids inhibit release of GABA by striatonigral axons and, moreover, depolarization of SNR neurons causes endocannabinoid-mediated suppression of GABAergic inhibitory postsynaptic currents. These data indicate that endocannabinoids mediate retrograde signaling from SNR neurons to the presynaptic CB_1-expressing axons of striatonigral neurons. Interestingly, because SNR neurons do not appear to express FAAH, the dynamics of retrograde endocannabinoid signaling at these synapses may be different to synapses where FAAH is expressed postsynaptically (e.g. hippocampal pyramidal cells) and further experimental analysis is now required to address this issue.

In conclusion, this study provides a neuroanatomical basis for future investigations of endocannabinoid signaling at synapses in many regions of the brain. In particular, our data suggest that the dynamics of endocannabinoid signaling may be directly influenced by the occurrence and relative abundance of FAAH in neurons. Moreover, the identification of FAAH-immunoreactive neurons without associated CB_1 cannabinoid receptor expression may pave the way for functional analysis of fatty acid amide signaling pathways mediated by other receptors.

Acknowledgements—This work was supported by a Wellcome Trust grant (057058) awarded to M.R.E. We are grateful to Kristin Demarest (TSRI) for technical assistance and to John Priestley (QMUL) for use of his digital photomicroscope. We are also grateful to Swidbert Ott (QMUL) for help and advice with digital photomicroscopy and to two anonymous reviewers for their constructive criticism of the manuscript.

REFERENCES

Breivogel CS, Griffin G, Di Marzo V, Martin BR (2001) Evidence for a new G protein-coupled cannabinoid receptor in mouse brain. Mol Pharmacol 60:155–163.

Carlson G, Wang Y, Alger BE (2002) Endocannabinoids facilitate the induction of LTP in the hippocampus. Nat Neurosci 5:723–724.

Cravatt BF, Prospero-Garcia O, Siuzdak G, Gilula NB, Henriksen SJ, Boger DL, Lerner RA (1995) Chemical characterization of a family of brain lipids that induce sleep. Science 268:1506–1509.

Cravatt BF, Giang DK, Mayfield SP, Boger DL, Lerner RA, Guilula NB (1996) Molecular characterization of an enzyme that degrades neuromodulatory fatty-acid amides. Nature 384:83–87.

Cravatt BF, Demarest K, Patricelli MP, Bracey MH, Giang DK, Martin BR, Lichtman AH (2001) Supersensitivity to anandamide and enhanced endogenous cannabinoid signaling in mice lacking fatty acid amide hydrolase. Proc Natl Acad Sci USA 98:9371–9376.

Dinh TP, Carpenter D, Leslie FM, Freund TF, Katona I, Sensi SL, Kathuria S, Piomelli D (2002) Brain monoglyceride lipase participating in endocannabinoid inactivation. Proc Natl Acad Sci USA 99:10819–10824.

Egertová M, Elphick MR (2000) Localisation of cannabinoid receptors in the rat brain using antibodies to the intracellular C-terminal tail of CB_1. J Comp Neurol 422:159–171.

Egertová M, Giang DK, Cravatt BF, Elphick MR (1998) A new perspective on cannabinoid signalling: complementary localization of fatty acid amide hydrolase and the CB_1 receptor in rat brain. Proc R Soc Lond B 265:2081–2085.

Egertová M, Cravatt BF, Elphick MR (2000) Fatty acid amide hydrolase expression in rat choroid plexus: possible role in regulation of the sleep-inducing action of oleamide. Neurosci Lett 282:13–16.

Elphick MR, Egertová M (2001) The neurobiology and evolution of cannabinoid signalling. Phil Trans R Soc Lond B 356:381–408.

Giang DK, Cravatt BF (1997) Molecular characterization of human and mouse fatty acid amide hydrolases. Proc Natl Acad Sci USA 94: 2238–2242.

Goparaju SK, Ueda N, Yamaguchi H, Yamamoto S (1998) Anandamide amidohydrolase reacting with 2-arachidonoylglycerol, another cannabinoid receptor ligand. FEBS Letters 422:69–73.

Gubellini P, Picconi B, Bari M, Battista N, Calabresi P, Centonze D, Bernardi G, Finazzi-Agro A, Maccarrone M (2002) Experimental Parkinsonism alters endocannabinoid degradation: implications for striatal glutamatergic transmission. J Neurosci 22:6900–6907.

Herkenham M, Lynn AB, Johnson MR, Melvin LS, de Costa BR, Rice KC (1991) Characterization and localization of cannabinoid receptors in rat brain: a quantitative *in vitro* autoradiography study. J Neurosci 11:563–583.

Holstege G, Blok BFM, ter Horst GJ (1995) Brain stem systems involved in the blink reflex, feeding mechanisms and micturation. In: The rat nervous system, 2nd edition (Paxinos G, ed), pp 257–275. San Diego: Academic Press.

Katona I, Rancz EA, Acsady L, Ledent C, Mackie K, Hajos N, Freund TF (2001) Distribution of CB_1 cannabinoid receptors in the amygdala and their role in the control of GABAergic transmission. J Neurosci 21:9506–9518.

Kreitzer AC, Regehr WG (2001a) Retrograde inhibition of presynaptic calcium influx by endogenous cannabinoids at excitatory synapses onto Purkinje cells. Neuron 29:717–727.

Kreitzer AC, Regehr WG (2001b) Cerebellar depolarization-induced suppression of inhibition is mediated by endogenous cannabinoids. J Neurosci 21:1–5 RC174.

Kreitzer AC, Regehr WG (2002) Retrograde signaling by endocannabinoids. Curr Opin Neurobiol 12:324–330.

Lichtman AH, Hawkins EG, Griffin G, Cravatt BF (2002) Pharmacological activity of fatty acid amides is regulated, but not mediated, by fatty acid amide hydrolase *in vivo*.. J Pharmacol Exp Ther 302:73–79.

Maejima T, Ohno-Shosaku T, Kano M (2001a) Endogenous cannabinoid as a retrograde messenger from depolarized neurons to presynaptic terminals. Neurosci Res 40:205–210.

Maejima T, Hashimoto K, Yoshida T, Alba A, Kano M (2001b) Presynaptic inhibition caused by retrograde signal from metabotropic glutamate to cannabinoid receptors. Neuron 31:463–475.

Matsuda LA, Bonner TI, Lolait SJ (1993) Localization of cannabinoid receptor mRNA in rat brain. J Comp Neurol 327:535–550.

Ohno-Shosaku T, Maejima T, Kano M (2001) Endogenous cannabinoids mediate retrograde signals from depolarized postsynaptic neurons to presynaptic terminals. Neuron 29:729–738.

Paxinos G, Franklin KBJ (2001) The mouse brain in stereotaxic cordinates, 2nd ed. London: Academic Press.

Shepherd GM, Greer CA (1998) Olfactory bulb. In: The synaptic organization of the brain, 4th edition (Shepherd GM, ed), pp 159–203. New York: Oxford UP.

Thomas EA, Cravatt BF, Danielson PE, Gilula NB, Sutcliffe JG (1997) Fatty acid amide hydrolase, the degradative enzyme for anandamide and oleamide, has selective distribution in neurons within the rat central nervous system. J Neurosci Res 50:1047–1052.

Thomas EA, Cravatt BF, Sutcliffe JG (1999) The endogenous lipid oleamide activates serotonin 5-HT_7 neurons in mouse thalamus and hypothalamus. J Neurochem 72:2370–2378.

Trettel J, Levine ES (2002) Cannabinoids depress inhibitory synaptic inputs received by layer 2/3 pyramidal neurons of the neocortex. J Neurophysiol 88:534–539.

Tsou K, Nogueron MI, Muthian S, Sañudo-Peña MC, Hillard CJ, Deutsch DG, Walker JM (1998) Fatty acid amide hydrolase is located preferentially in large neurons in the rat central nervous system as revealed by immunohistochemistry. Neurosci Lett 254: 137–140.

Wallmichrath I, Szabo B (2002) Cannabinoids inihibit striatonigral GABAergic neurotransmission in the mouse. Neuroscience 113: 671–682.

Wilson RI, Nicoll RA (2001) Endogenous cannabinoids mediate retrograde signalling at hippocampal synapses. Nature 410:588–592.

Wilson RI, Nicoll RA (2002) Endocannabinoid signaling in the brain. Science 296:678–682.

Wilson RI, Kunos G, Nicoll RA (2001) Presynaptic specificity of endocannabinoid signaling in the hippocampus. Neuron 31:1–20.

(Accepted 20 January 2003)